Moroccan Journal of Chemistry
ISSN: 2351-812X
http://revues.imist.ma/?journal=morjchem&page=login
Aoumeur & al. / Mor. J. Chem. 9 N°1 (2021) 274-289

Molecular docking studies for the identifications of novel antimicrobial compounds targeting of staphylococcus aureus

Nabila Aoumeur [(a)], Nourddine Tchouar [(a)], Salah Belaidi [(b)], Mebarka Ouassaf [(b)], Touhami Lanez [(c)], Samir Chtita[(d)]*

[(a)] Laboratory of Process Engineering and Environment, Faculty of Oran, University of Sciences and Technologies of Oran (MB-USTO), BP150, 31000, Oran, Algeria.
[(b)] Laboratory of Molecular Chemistry and Environment, Group of Computational and pharmaceutical Chemistry, University of Biskra, BP145, 07000, Biskra, Algeria.
[(c)] Valorization and Technology of Sahara Resources Laboratory, University of El Oued, BP. 789, 39000, El Oued, Algeria.
[(d)] Laboratory of Physical Chemistry of Materials, Faculty of Sciences Ben M'Sik, Hassan II University of Casablanca, BP. 7955 Sidi Othmane, Casablanca, Morocco.

** Corresponding author:*
samirchtita@gmail.com
Received 05 March 2020,
Revised 23 Dec 2020,
Accepted 01 May 2021

Abstract

This work include several advanced molecular docking tools to study the interactions of our newly synthesized 1,3,4-thiadiazole derivatives in the active site of penicillin binding protein and DNA gyrase against Staphylococcus aureus, the enzymes targeted for antimicrobial agents. Results such as MolDock scores, binding energies, residue binding distances, etc. were identified and discussed in this present research. The molecules with best docking results were selected in order to calculate drug likeness and bioavailability using Molinspiration software. All the compounds obey Lipinski's rule and its extension and showed drug likeness. The pharmacokinetic parameters study was done using the AdmetSAR to display ADME and toxicity properties of these antimicrobial.

Keywords: *1,3,4-thiadiazole, NPHACT, NPHADMT, Antimicrobial, Molecular docking, Staphylococcus aureus.*

1. Introduction

Recently, bacterial have increased dramatically. Finding the adequate treatment is a real challenge because of the deficiency of many procedures due to the emergence of multiple-drug-resistance organisms and the acquired immune deficiency syndrome (AIDS) pandemic [1, 2]. The most common germs are Staphylococcus (Gram-positive), which are a potent pathogen for nosocomial infections [3]. The bacteria which move into the bloodstream may cause bacteremia and infect almost all the parts of the body, especially the heart valves (endocarditis) and bones (osteomyelitis). Proteins continue to assume significant attention from the pharmaceutical and biotechnology industries as a valuable source of potential drug targets [4]. Bacterial cell division and daughter cell formation are complex mechanisms whose details are orchestrated by at least a dozen different proteins. Penicillin-binding proteins (PBPs), membrane-associated macromolecules which play key roles in the cell wall synthesis process [5]. The most important clinically used inhibitors of PBPs are β-lactams which inhibit transpeptidase activity of PBPs by forming a covalent penicilloyl-enzyme complex that blocks the normal transpeptidation reaction; this finally results in bacterial death. Another well studied target in the Gram-positive bacterial infections includes the Type DNA gyrase. It plays a critical role in bacterial cell survival that controls the topology of DNA during processes of transcription, replication and recombination by introducing transient breaks to both DNA strands [6, 7] Thiadiazole is a 5-membered heterocyclic ring system containing two nitrogen and one sulphur atoms. 1,3,4- thiadiazole present many interests because of their versatile biological actions; In particular, compounds bearing the 1,3,4-thiadiazole nucleuses are known as interesting derivatives in all aspects of drug discovery [8]. These compounds have other interesting activities such as: antimicrobial, anti-inflammatory, analgesic, anti-tumors, antiviral, antifungal and antitubercular agents [9-16]. A new series of 1,3,4-thiadiazoles derivatives synthesized in our laboratory from (2,4-dichlorophenoxy) acetyl chloride and 3-chloro-2-chlorocarbonylbenzo [b] thiophene (shown in Table 1) as bacteria Staphylococcus aureus, inhibitor is considered in this study [17]. Several co-crystallized structures for Staphylococcus aureus were carried out with different inhibitors, makes it possible to apply a molecular docking protocol to explore the enzyme-inhibitor interactions. We applied molecular dynamics (MD) [18-20], which is represents the flexibility of both the ligand and protein more effectively than other algorithms [21]. Therefore we use the molecular docking study because it is extremely significant in a wide range of applications in computer aided drug designing. The no covalent binding interaction between a macromolecule (receptor) obtained from protein data banks, and a small molecule (ligand) may result in activation or inhibition of the enzyme [22]. The docking process involves prediction of the ligand conformation as well as its position and orientation within these sites (usually referred to as pose) and assessment of the binding affinity [23]. In this study, two biological macromolecule enzymes: Penicillin binding proteins (PBPs), and DNA gyrase, which were needed by bacteria in the process of biosynthesis, was chosen as target molecules. In this way we are able to find out the potential of our synthesized compounds against Gram positive bacteria. Furthermore, it was considered logical to perform a drug likeness evaluation and computational prediction of pharmacokinetic parameters using Molinspiration and AdmetSAR online softwares [24].

2. Materials and methods

2.1. Antimicrobial activity

The tested compounds were evaluated in vitro antimicrobial activity against bacterial and fungal species, gram-negative bacteria strain Escherichia coli (E. coli), and gram-positive bacteria strain Staphylococcus aureus (S. aureus), two fungi strain Mucor sp and Penicillium sp using paper disc diffusion technique and expressed as the diameter of the inhibition zones according to the agar plate diffusion method [17]. The sterilized medium [25] was inoculated with the suspension of the microorganism and poured into Petri dish (3-4 mm depth) [26, 27], and expressed as the

diameter of the inhibition zones according to the agar plate diffusion method. One ml of each sample (at 0.5 mg/ml) was added to each well (10 mm diameter holes cut in the agar gel) [28]. The plates were incubated for 24 h at 37 °C (for bacteria and yeast) and for 72 h at 27 °C (for filamentous fungi) [17]. After incubation, the microorganism's growth was observed. Tetracycline was used as a standard for the antibacterial activity, while amphotericin B for the antifungal activity. The resulting inhibition zone diameters were measured in millimeters and used solvent controls DMF (Dimethyleformamide) were included in every experiment as negative controls, confirming that it has no influence on the growth of the tested microorganisms. The compounds below have been considered important ligands as inhibitors against microbial activity in terms of expulsion. All the tested compounds exhibit almost identical activities against bacterial and fungal activities, as reflected by the values of the diameters of their zones of inhibition (Table 1).

Table 1: The inhibition zones (IZ) in mm diameter of the synthesized compounds on antibacterial species

Compound N°.	Name of the compound	Diameter of inhibition zone (mm) Staphylococcus aureus
ACT	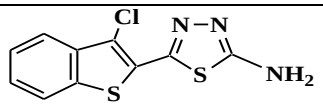 L_1 2-amino-5-(3-chlorobenzo[b]thien-2-yl)-1,3,4-thiadiazole	12
NPHACT	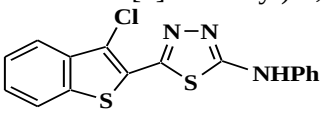 L_2 5-(3-chlorobenzo[b]thien-2-yl)-2-(N-phenylamino)-1,3,4-thiadiazole	18
ADMT	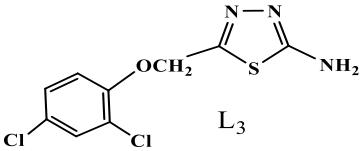 L_3 2-amino-5-[(2,4-dichlorophenoxy)methyl]-1,3,4-thiadiazole	10
NPHADMT	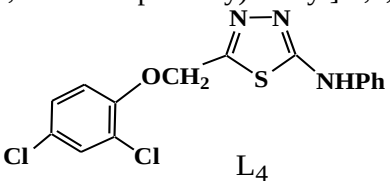 L_4 5-[(2,4-dichlorophenoxy)methyl)-2(Nphenylamino)-1,3,4 thiadiazole	08

2.2. Ligands Structure optimization

All ligand structures of 1,3,4-thiadiazole derivatives [17] were optimized using MM+ molecular modeling and the semi-empirical AM1 methods, both methods are implemented in HyperChem 8.08 software [29]. For these calculations, the "Steepest Descent", conjugate gradient algorithm was employed, with the RMS gradient set to 0.01 kcal/(Å.mol). The resulting structures were saved in ".mol" file formats for molecular docking studies. In the next step, we carried out MD simulations to predict the binding mode of these compounds. The aim of MD simulations was

to obtain ligand-protein structures closer to physiological conditions and to examine conformational and dynamical variation of the enzyme upon ligand binding [30, 31]. The molecular structures was minimized over 1500 steps (at 0 K), the equilibration protocol consisted of 1000 minimization steps, followed by 30 ps of MD simulations at 10 K with fixed protein atoms, then, we gradual heating from 10 to 310 K with a step of integrations of 1 fs. In this case geometrical parameters calculated through the 500 ps-long MD simulations of ligands [32, 33], are presented in Figure1.

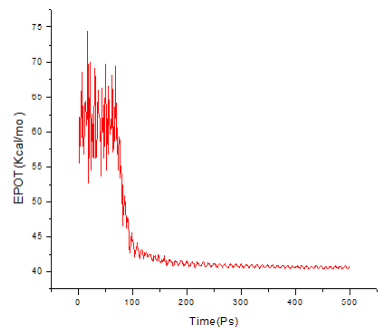

(ACT)

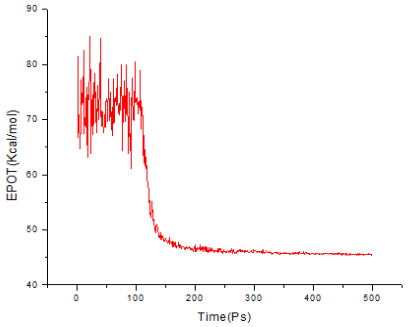

(NPHACT)

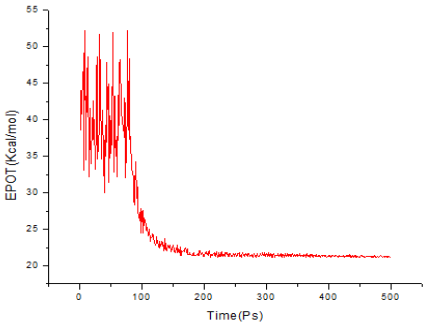

(ADMT)

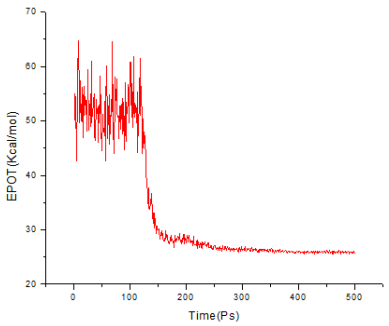

(NPHADMT)

Figure 1: Variation of the potential energy of the ligands as a function of time

2.3. Enzyme Structure

The X-ray structure of S. aureus DNA Gyrase B, was downloaded from the Protein Data Bank (PDB ID: 3G75) [34]. It is co-crystallized with inhibitors 4-methyl-5-[3-(methylsulfanyl)-1H-pyrazol-5-yl]-2-thiophen-2-yl-1,3-thiazole C12H11N3S3 the heteroatom's and coordinates are removed from the PDB file. The three-dimensional structure of 3G75 was obtained by X-ray diffraction in complex with a selective inhibitor thiazole with EC Number: 5.6.2.2 chains (A, B), resolution 2.30 Å, and R-value 0.244. In this study we have taken a chain A, 184 residues and 2898 atoms. This allowed us to obtain the model shown in Figure 2. The crystal structure of penicillin-binding protein 3 (PBP3) from methicilin-resistant staphylococcus aureus in the cefotaxime bound from C14H15N5O5S2 (PDBID: 3VSL) [34] was downloaded from RCSB Database (http://www.rcsb.org/pdb)

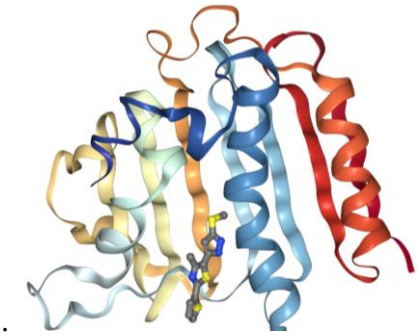

Figure 2: Three-dimensional crystal structure of the target enzyme (3G75)

Enzyme 3VSL is a three-dimensional structure with chains (A, B), resolution 2.40 Å, and R-value 0.247. In this study we have taken a chain A, 631 residues and 9937 atoms. This allowed us to obtain the model shown in Figure 3.

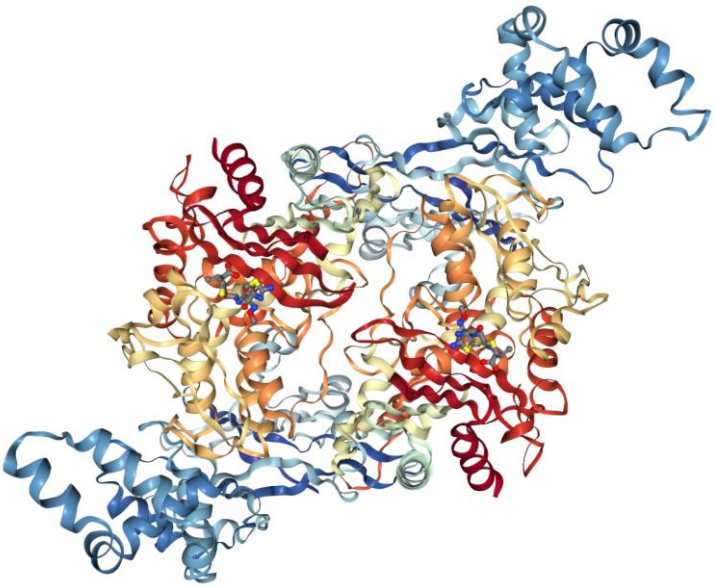

Figure 3: Three-dimensional crystal structure of the target enzyme (3VSL)

2.4. Molecular Docking

Molegro Virtual Docker (MVD2012) software [35], is advanced docking analysis software used to predict protein-ligand interactions. In the present investigation, we make use of a docking algorithm called MolDock. So, MolDock is based on a new hybrid search algorithm, called guided differential evolution. The guided differential evolution algorithm combines the differential evolution optimization technique with a cavity prediction algorithm. The use of predicted cavities during the search process, allows for a fast and accurate identification of potential binding modes (poses). We used MVD because it showed higher docking accuracy than other stages of the docking products (MVD: 87%, Glide: 82%, Surflex: 75% and FlexX: 58%) in the market [36, 37]. This molecular docking protocol generate five best predicted poses for each 1,3,4-thiadiazole compound with Moldock score, Rerank score, and Hydrogen bond score. The docked conformations or pose with the minimum MolDock score values is the optimal pose [37]. The Re-Ranking score function is generally more reliable than the MolDock score function at selecting the best solution among multiple solutions derived from the same ligand [38]. A schematic 2D representation of protein-ligand complex was generated by LigPlot+ [39], a graphical system of automatically generating multiple 2D diagrams of ligand protein interactions from 3D coordinates.

2.5. Cavity prediction

In this silico analysis, a maximum of cavities was detected using default parameters, to obtain binding sites in the DNA gyrase protein (PDB ID: 3G75), and Penicillin Binding Protein (PDB ID: 3VSL) in Figure 4 and Figure 5. The cavities within a 30 x 30 x 30 $Å^3$ cube centered at the experimentally known ligand position were used. From these predicted cavities (Table 1 and 2) the one with the highest volume (31.232 $Å^3$, of 3G75 and 231.9 $Å^3$ of 3VSL) and surface (106.69 $Å^2$ of 3G75 and 660.48 $Å^2$ of 3VSL), was selected for consideration, as it includes the bound ligand.

Table 2: Cavity information of enzymes (3G75.pdb) and (3VSL.pdb)

Enzymes	Cavity Name	Volume ($Å^3$)	Surface Area ($Å^2$)
3G75	Cavity 1	031.23	106.24
	Cavity 2	026.11	112.64
3VSL	Cavity 1	231.90	660.48
	Cavity 2	151.50	533.76
	Cavity 3	107.00	428.80
	Cavity 4	065.04	264.96
	Cavity 5	034.30	119.04

The binding site was set inside a restriction sphere of 15 radiuses with the center X: 49.95, Y: -6.21, Z: 20.91 for (3G75) enzyme and X: 16.48, Y: -47.79, Z: 25.5 for (3VSL) enzyme. The MolDock grid score was set with a grid resolution of 0.30 Å and for each of the 10 independent runs; a maximum number of 1500 interactions were executed on a single population of 50 individuals.

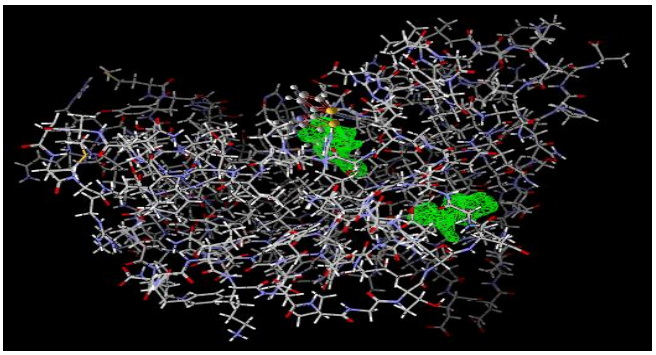

Figure 4: The two MVD- detected cavities in gyrase B protein, PDB code of 3G75
Detected cavities in green, carbon atom in grey, oxygen atoms in red and nitrogen atoms in blue

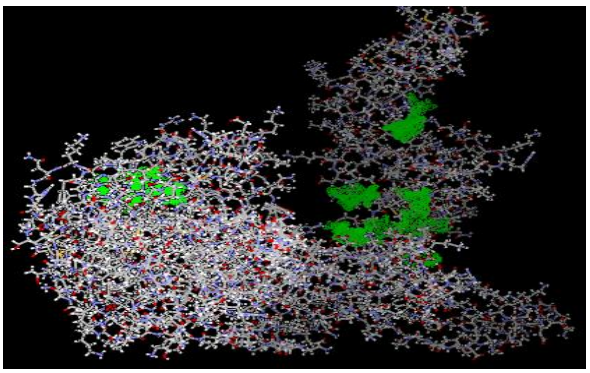

Figure 5: The five MVD-detected cavities in penicillin binding protein, PDB code of 3VSL
Detected cavities in green, carbon atom in grey, oxygen atoms in red and nitrogen atoms in blue

2.5. Evaluation of drug likeness

The utility of drug ability from a medicinal chemistry standpoint has been summarized by the rule of five (Lipinski rules, Ro5) and its extensions [40]. The drug likeness was evaluated through the Lipinski, Ghose and Veber rules using Molinspiration online molecular property calculation toolkit [41, 42]. (http://www.molinspiration.com/cgi-bin/properties)

2.6. ADME & Toxicity Studies

The ADMET properties of the molecules were predicted by using AdmetSAR (http://lmmd.ecust.edu.cn) for assessing the disposition and potential toxicity of ligand with in an organism [43].

3. Results and Discussions

3.1. Protein-Ligand Docking

The Protein-Ligand interaction plays a vital role in structural based drug design. Computational analysis was carried out on chain A of the enzyme 3G75 and 3VSL. The 4 ligands were selected for the study of the protein-ligand interactions, five top poses for each ligand were returned in the simulation, out of which one best pose for each ligand was selected on the basis of their MolDock score. The MVD score and the re-ranks cores and H-Bound score (Kcal/mol), for each docking studies of 1,3,4-thiaidazole ligands with 3G75 and 3VSL are summarized in the Table 3.

3.2. Antibacterial interaction: (3G75, 3VSL)-Ligands

The obtained results show that all the ligands have interactions with the 3G75 and 3VSL at the level of the cavity 1 (Figure 4 and Figure 5), corresponding are listed in Table 2, shown in terms of based essentially on the comparison between the obtained energies using Mol Dock Score (GRID), and the obtained results during molecular docking, it is noted that the energies of the complexes formed by ligands L2, L4, with the two proteins (3G75 and 3VSL) are lower compared to other complexes (Table 3).Those four top-ranked ligands will form more stable complex and be better able to inhibit and reduce the activity of S. aureus.

Table 3: Docking results of 3G75 and 3VSL enzymes with of the compounds studied

	3G75				3VSL			
Ligands	Moldock score (Kcal/mol)	Interaction (Kcal/mol)	H-bound (Kcal/mol)	Rerank score (Kcal/mol)	Moldock score (Kcal/mol)	Interaction (Kcal/mol)	H-bound (Kcal/mol)	Rerank score (Kcal/mol)
1	-108.384	-105.006	-2.361	-84.991	-102.525	-100.815	-7.125	-80.938
2	-133.409	-134.647	-0.826	-88.217	-120.551	-120.325	-6.144	-97.432
3	-109.119	-112.366	-0.164	-83.712	-103.604	-111.189	-8.240	-72.440
4	-127.059	-135.535	-0.911	-62.052	-133.150	-139.742	-4.223	-107.189

In addition, the docking results of the interactions between compounds and receptor can be analyzed by means of visualization using Molegro molecular viewer program. Visualization helps to observe amino acid residues contact and the hydrogen bonds formed between the ligand and the receptor [44]. The number and length of hydrogen bonds the amino acid residues that interact with receptors of the compounds are shown in Figure 6 and Figure 7.

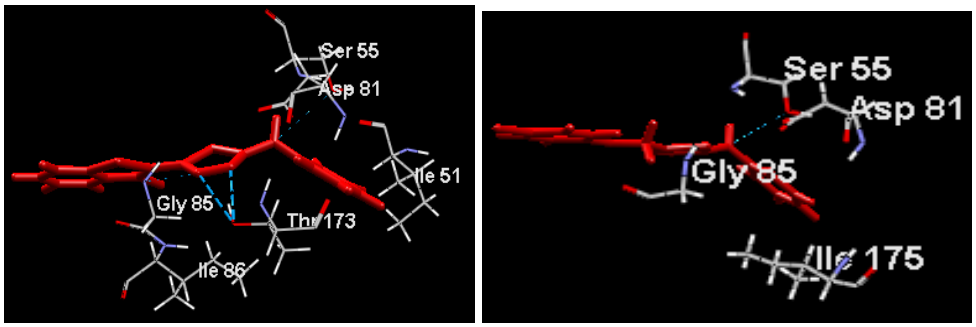

Figure 6: Hydrogen bonds interaction between NPHACT (left) and NPHADMT (right), and residues of active site of 3G75

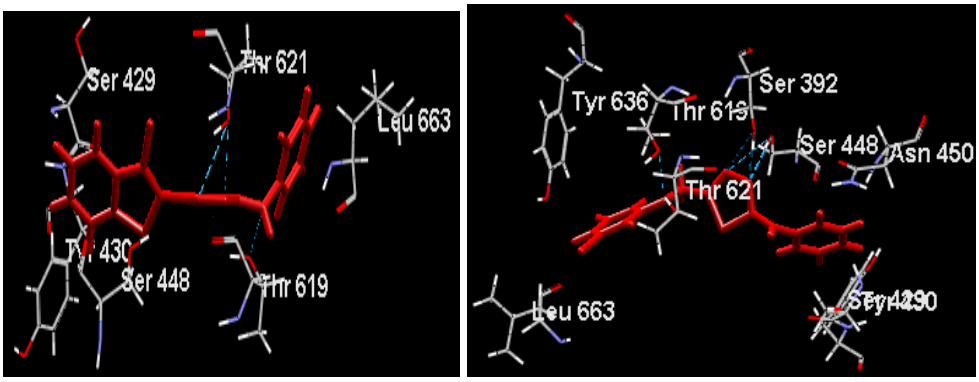

Figure 7: Hydrogen bonds interaction between NPHACT (left) and NPHADMT (right), and residues of active site of 3VSL

Table 4: Prediction interactions with DNA gyrase binding site

Interacting residues of receptor 3G75	Interaction	distance (Å)	Interaction strength (Kcal/Mol)
NPHACT	H- bond		
	Thr173……..N	2.80	-2.50
	Thr173...……..N	3.01	-2.50
	Ser55…..……N	3.33	-0.34
	Ile86……NH	3.46	-0.31
	Steric		
	Gly85…..S	2.66	3.90
	Ile51..…..…C	2.69	3.70
	Asp81…….....C	2.36	5.71
	Asp81……C	2.82	2.93
NPHADMT	H- bond		
	Ser55...…..NH	3.16	-0.91
	Steric		
	Gly85.……..C	2.74	3.42
	Ile175……...C	3.19	0.64
	Asp81……...C	3.08	1.33
	Asp81…….....C	2.60	4.27
	Ser55…….....C	3.12	1.08

The docked structure of NPHACT indicated that the nitrogen atom was extensively hydrogen bonded to the Thr173 two bond, and Ser55 residues with bond distances of (2.86, 3.01 Å), and 3.33 Å respectively (Table 4) (Figure 8). Another nitrogen atom (N-H) group of compound NPHACT was also involved in a hydrogen bond interaction with the Ile86 residue of the 3G75. Additionally, Gly85, Ile51, and Asp81 residues of the 3G75 displayed strong steric interactions with compound NPHACT. The interactions with distances between 2.5 Å and 3.1 Å are considered strong, although those with distances between 3.1 Å and 3.55 Å are assumed to be average and when their distances are greater than 3.55 Å, they are considered to be weak. It is noticed that the values obtained for distances between the residues of the active site and the NPHACT, NPHADMT vary between 2.66 Å and 3.46 Å [44, 45]. Other residues of 3G75, Arg84, Arg144, Glu58, Pro87, Ile75, Val79, Asn54, and Pro87, demonstrated hydrophobic interactions with compound NPHACT (Figure 9). The compound NPHADMT bearing 2,4-dichlorophenoxyacetic showed the second best ligand. The stereo view of the docked complex indicated that the compound NPHADMT was extensively hydrogen bonded with the Ser55 residue of the 3G75 (Figure 8). NPHADMT share generally the amino acids residues shows that Val79, Thr173, Ile51, Glu58, Asn54, Ile86, Pro87, Arg84 and Arg144 are involved in hydrophobic contacts, Figure 9.

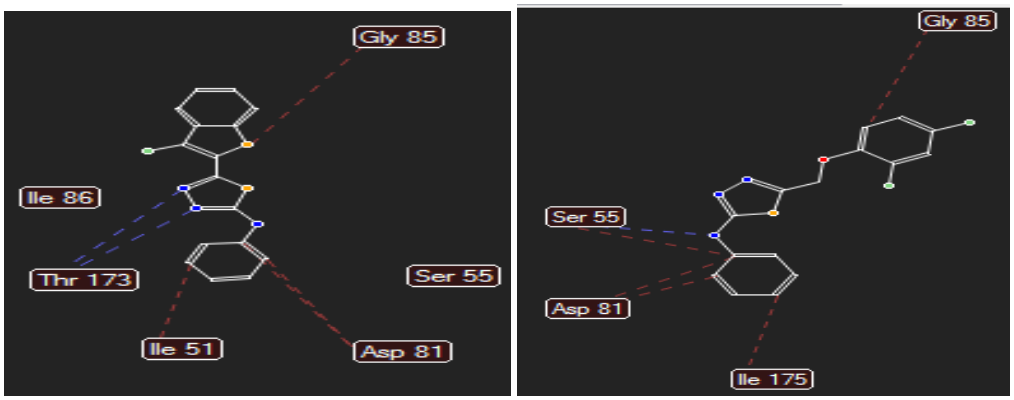

----: Interactions steric. ----: Interactions H-bond

Figure 8: Hydrogen bonding and steric interactions between Staphylococcus aureus receptor (DNA gyrase) and most active compounds; NPHAT (left) and NPHADMET (right)

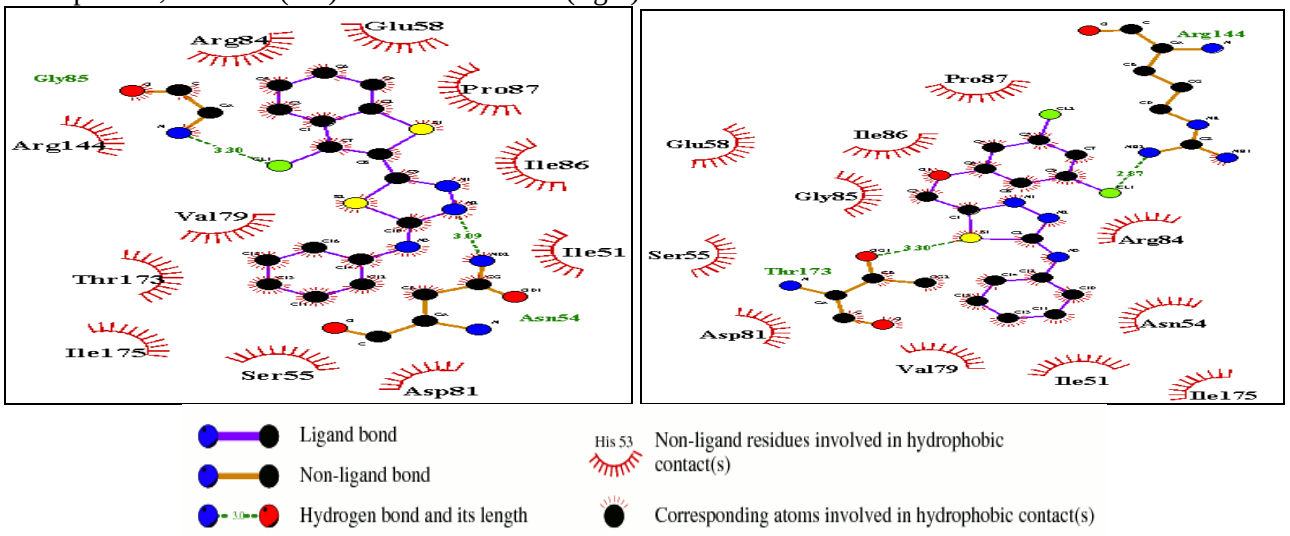

Figure 9: Ligplot+ results showing the interactions of most active compounds with 3G75 NPHACT (in the left) and NPHADMT (in the right)

LigPlot+ is known as the comprehensive tool for expressing the hydrogen bonding and hydrophobic interactions involving the ligand molecule and active site residues (Figure 10) gives a more detailed insight of the interactions with particular amino acids in enzyme binding pocket. NPHACT (Figure11 and Table 5) formed two strong H-bond with a distance radius of 2.74 Å, 3.11 Å to Thr621, and weak H-bond: 3.33 Å in the active site. It made six alkyl hydrophobic contacts with the residues Tyr430 (2), Ser429, Thy621 and Leu663 (2). In 3VSL (Figure 11), the ligand NPHADMT formed six H-bond with a distance (3.01Å, 3.30Å), (2.92 Å, 3.25 Å), 2.86 Å and 2.60Å to the residues Ser448 (2), Ser392 (2), Thr619 and Thr621 respectively. It formed eight alkyl hydrophobic contacts with the residues Thr430 (2), Asn450, Ser429, Leu663, Tyr636, Tyr619 (2).

Table 5: Prediction interactions with penicillin binding protein

Interacting residues of receptor 3VSL	Interaction	distance (Å)	Interaction strength (Kcal/Mol)
NPHACT	H- bond Tyr621……..N	2.74	-0.70
	Tyr621……..N	3.11	-1.83
	Thr619……NH	3.33	-0.52
	Steric Tyr430……..…C	3.12	1.07
	Tyr430…...…...C	3.18	0.70
	Ser429…...……C	3.03	1.60
	Ser448……...C	3.16	0.85
	Leu633…..……..C	2.73	3.44
	Leu633……...C	3.17	0.78
NPHADMT	H- bond Ser448……..N	3.01	-2.50
	Ser448……..N	3.30	-1.28
	Ser392……..…N	2.92	-2.50
	Ser392……...…N	3.25	-1.46
	Thr621…....…O	2.60	-0.70
	Thr619…...…...O	2.86	-077
	Steric Asn430……..C	2.19	2.39
	Asn430……..C	3.09	1.27
	Asn450……..…C	3.12	1.10
	Ser429……...…C	3.05	1.53
	Thr619…....…C	2.29	6.10
	Thr619…...…...C	3.12	1.12
	Leu633……..C	2.91	2.37
	Tyr636……...C	2.93	2.25

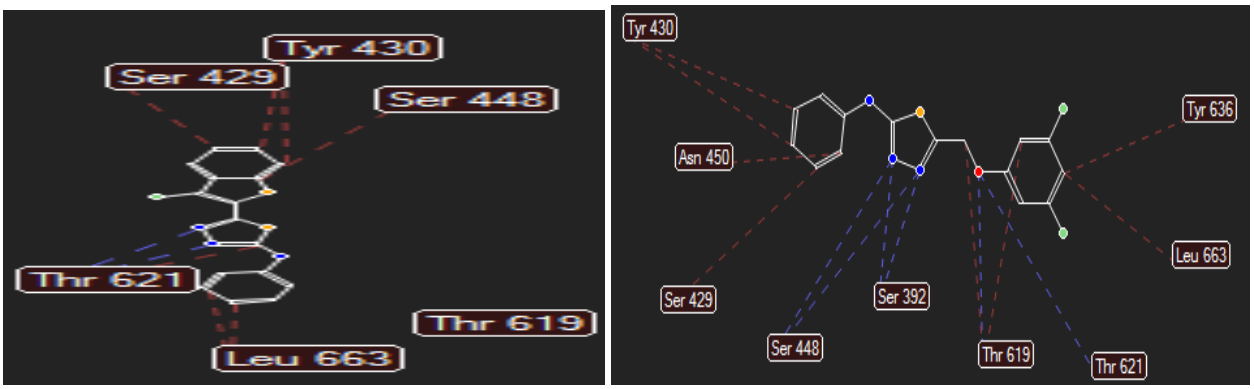

----: steric Interactions. ----: H-bond Interactions

Figure 10: Hydrogen bonding and steric interactions between Penicillin Binding Protein 3 receptor and most active compounds; NPHAT (left) and NPHADMET (right)

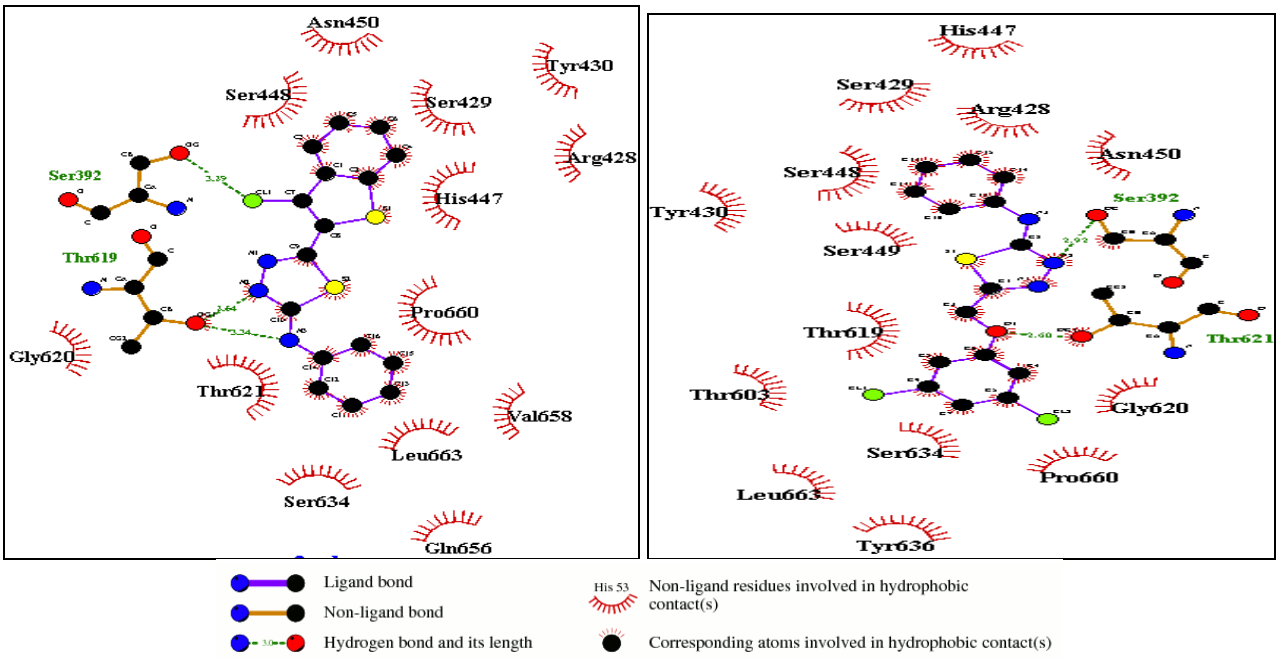

Figure 11: Ligplot+ results showing the interactions of most active compounds with 3VSL NPHACT (in the left) and NPHADMT (in the right)

Based on the presented results, it can be concluded that hydrophobic interactions between NPHACT, NPHADMT and binding pocket play an important role. However, number, bond length and bond energy of hydrogen bonds formed between ligand and enzyme has an important role in ligand effect on investigated activity. Most of amino acid residues in hydrophobic active site were involved in affinity hydrophobic bonding interactions of ligand [36, 39] (Figure 12 and Figure13). These figures show hydrophobic and electrostatic bonding between the most active compounds NPHACT and NPHADMT with 3G75 and 3VSL. The structure of most main content of 1, 3,4-thiadiazole was no polar, so this gave an advantage to hydrophobic for binding inside chains as receptor active site. The result shows that NPHACT and NPHADMT binds effectively to the receptor enzymes 3G75, 3VSL when compared to the other derivatives from 1,3,4-hiadiazole with a docking energy score of -133.409, -120.551, -127.059and -133.150 Kcal/mol respectively. We suggest that 5-(3-chlorobenzo[b]thien-2-yl)-2-(N-phénylamino)-1,3,4-thiadiazole and 5-[(2,4-dichlorophenoxy) methyl)-2(Nphenylamino)-1,3,4 thiadiazole could be investigated further using in vitro models for

its anti-bacterial activity and other pharmacological properties. All the obtained results at the theoretical level as well as that of the biological activity confirm the interest of our 1, 3,4-thiadiazole derivatives which is the originality of our work. The compounds have different inhibitory could further analyzes with different mechanism.

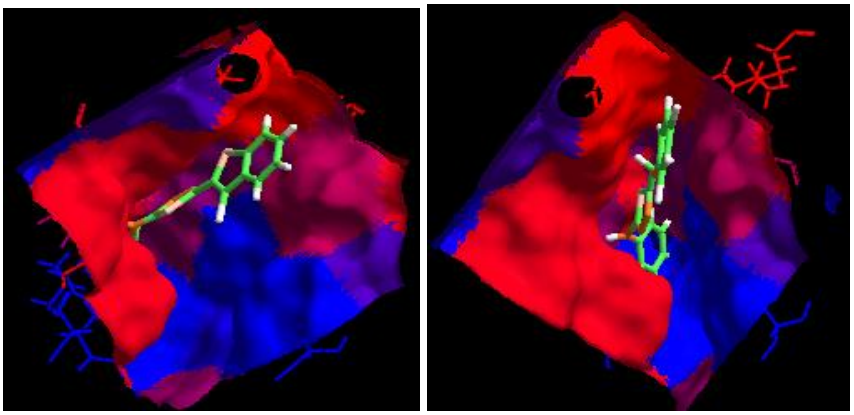

Figure 12: Hydrophobic bonding interactions between 3G75and most active compounds NPHACT (in the left) and NPHADMT (in the right)

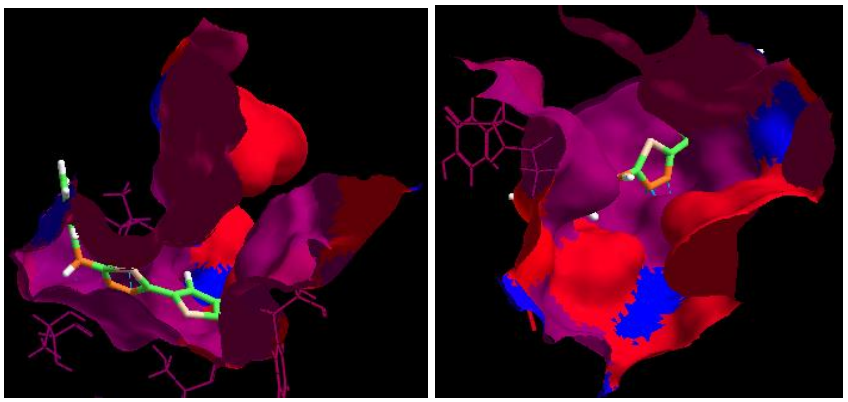

Figure 13: Hydrophobic bonding interactions between 3VSL and most active compounds NPHACT (in the left) and NPHADMT (in the right)

3.3. Drug likeness and ADMET studies

The results from Table 6 reveal the two compounds NPHACT and NPHADMT. Obeyed the Lipinski, Veber and Ghose rules they showed a good drug likeness score. We were found that they show zero violation of the rules.

That molecules have logP ≤ 5, molecular weight ≤500, number of hydrogen bond acceptors ≤10, and number of hydrogen bond donors ≤ 5, topological polar surface area (TPSA) < 140 $Å^2$ and number of rotatable bonds (n rotb) < 10 this measures molecular flexibility and also, the total number of atoms between (N.A.) 20 and 70.

Table 6: Lipinski properties of plant compounds analyzed using Molinspiration

S. N°	Compound	M.W	Log P	H-bond D	H-bond A	TPSA	N.RotB	N.A
L2	NPHACT	343.86	1.82	1	5	37.81	3	22
L4	NPHADMT	352.25	1.76	1	5	47.05	5	22

Notes: log P: partition coefficient; TPSA: Topological polar surface area; N.A: number of atoms; MW: molecular weight; H-bond A: number of hydrogen acceptor; H-BOND D: number of hydrogen donor, N.RotB: number of rotatable bonds.

ADMET properties, as derived from AdmetSAR server, reveal that NPHACT and NPHADMT had good Human Intestinal Absorption (HIA) score. Greater HIA denotes that the compound could be better absorbed from the intestinal tract upon oral administration. The penetration through the Blood-Brain Barrier (BBB) came out to be below 1 (CBrain/CBlood < 1) are classified as inactive in the CNS. The penetration of the blood brain barrier is critical in the pharmaceutical field, because compounds that act on the central nervous system (CNS) should go through it, and inactive compounds in CNS, Should not go in order to avoid collateral effects of CNS [46]. One of the important reasons for the discovery of new drugs is the evaluation of the toxicity of drug candidates, is very important to predict the mutagenicity and carcinogenicity of new compounds that may be toxic.

Table 7: ADMET properties of the ligands

S. N°	Compound	HIA	BBB	AMES toxicity	Carcinogenicity	LD_{50} in rat (mol/kg)
2	NPHACT	1.0000	0.9347	Non-toxic	Non-carcinogen	2.6589
4	NPHADMT	0.9935	0.9627	Non-Toxic	Non-carcinogen	2.4143

In the prediction of carcinogenicity in rat, the compounds NPHACT and NPHADMT had negative prediction; the Salmonella Ames assay is one of the most widely used short-term basic regulatory tests to assess the mutagenic potential of new chemical entities. The two compounds were AMES negative. The results of the two compounds are described in Table 7, and their high LD50 values (2.65; 2.45) suggest that the compounds are lethal only at very high doses.

4. Conclusion

From this study of molecular docking on 1,3,4-thiadiazole derivatives, we conclude that those derivatives have the ability to inhibit the bacterial species staphylococcus aureus with different mechanism. The molecules NPHACT and NPHADMT have the best poses, with the higher negative mol dock score, rerank score and hydrogen bond interaction with receptor PBP3 and, DNA gyrase. The research has shown that the two ligands act as possible binding sites for the design of more selective and targeted molecule against (3G75, 3VSL) in the active site (the cavity 1).

The obtained compounds showed excellent drug-likeness, all pharmaco-kinetic parameters of the NPHACT and NPHADMT were found to be within the range or are the recommended values to become a potent Inhibitor, these compounds can be analyzed by further in vitro studies and can be a lead in the designing of potential as antibacterial drug.

References

[1] Hardman, J.G., Limbird, L.E., Molinoff, P.: The pharmacological basis of therapeutics, 11ed McGraw-Hill, New York, **2006**.

[2] Salih, N., Salimon, J., Yousif, E.: Synthesis, characterization and antimicrobial activity of some carbamothioyl-1,3,4-thiadiazole derivatives, *International Journal of Pharmaceutical* Sciences *and Research*, **2012**, **4** ,655-660.

[3] Bhakdi, S., Tranum-Jensen, J.: Alpha-toxin of Staphylococcus aureus, *Microbiological reviews*, **1991, 55**,733-751.

[4] Deisenhofe, J., Smith, J.L., *Current Opinion in Structural Biology*, **2001**, **11**,701.

[5] Macheboeuf , P., Contreras-Martel , C., Job , V., Dideberg, O., Dessen, A.: Penicillin binding proteins: key players in bacterial cell cycle and drug resistance processes, *FEMS Microbiology Reviews*, **2006**, **30**,673–691.

[6] Tomašič, T., Mašič, L.P.: Prospects for developing new antibacterials targeting bacterial type IIA topoisomerases, *Current Topics in Medicinal Chemistry*, **2014**, **14**,130-151.
[7] Champoux, J.J.: DNA topoisomerases: Structure, function, and mechanism, *Annual Review of Biochemistry*, **2001**, **70**, 369-413.
[8] Mishra, G., Singh, A.K., Jyoti, K.: Review article on 1,3,4-Thiadiazole derivatives and its Pharmacological activities, *International Journal* of *ChemTech Research*, **2011**, **3** ,1380-1393.
[9] Turan-Zitouni, G., Kaplancikli, Z.A., Erol, K., Kilic, F.S.: Synthesis and analgesic activity of some triazoles and triazolothiadiazines, *Journal of Science Direct Il Farmaco*, **1999**, **54**, 218-223.
[10] Al-Soud, Y.A., Al-Masoudi, N.A., El-Ferwanah, A.: Synthesis and properties of new substituted 1,2,4-triazoles: Potential antitumor agents, *Bioorganic and Medicinal Chemistry*, **2003**, **11**, 1701-1708.
[11] Holla, B.S., Sarojini, B.K., Rao, B.S., Akberali, P.M. , Kumari, N.S., Shetty, V.: Synthesis of some halogen-containing 1,2,4-triazolo-1,3,4-thiadiazines and their antibacterial and anticancer screening studies, *Journal of ScienceDirect Il Farmaco*, **2001**, **56**, 565-570.
[12] Prakash, O., Bharadwaj, V. , Kumar , R., Tyagi, P. , Aneja, K.R.: Organoiodine (III) mediated synthesis of 3-aryl/hetryl-5,7- dimethyl-1,2,4-triazolo[4,3-a]pyrimidines as antibacterial agents, *European Journal of Medicinal Chemistry*, **2004**, **39**, 1073-1077.
[13] Foroumadi, A., Mansouri, S., Kiani, Z., Rahmani, A.: Synthesis and in vitro antibacterial evaluation of N-[5-(5-nitro-2-thienyl)-1,3,4-thiadiazole-2-yl] piperazinyl quinolones, *European Journal of Medicinal Chemistry*, **2003**, **38**, 851-854.
[14] He, R., Chen, Y., Ougolkov, A.V., Zhang, J-S., Savoy, D.N., Billadeau, D.D., Kozikowski, A.P.: Synthesis and biological evaluation of triazol-4-ylphenyl-bearing histone deacetylase inhibitors as anticancer agents, *Journal of Medicinal Chemistry*, **2010**, **53**, 1347-1356.
[15] Tarmas, S., Geza, S., Jozsef, R., Laszlo, P., Tibor, L., Lajos, T., Stephen, H.: New acylated 1,2,4-triazoles as antiviral agents, *Archiv der Pharmazie - Chemistry in Life Sciences*, **2006**, **319**, 238-242.
[16] Malladi, S., Isloor, A.M, Shetty, P.,Fun, H.K., Telkar, S., Mahmood, R., Isloor, N.: Synthesis and anti-inflammatory evaluation of some new 3,6-disubstituted-1,2,4-triazolo-[3,4-b]-1,3,4-thiadiazoles bearing pyrazole moiety, *Medicinal Chemistry Research*, **2012**, **21**, 3272-3280.
[17] Aoumeur, N.: Synthesis of penta-atomic nitrogen-containing heterocycles from hydrazine derivatives, Biological Application, Thesis of magister, USTO University, 2011.
[18] Brooks, B.R., Bruccoleri, R.E., Olafson, B.D., States, D.J., Swaminathan, S., Karplus, M.: A program for macromolecular energy, minimization, and dynamics calculations, *Journal of Computational Chemistry*, **1983**, **4**, 187-217.
[19] Cornell, W.D., Cieplak, P., Bayly, C.I., Gould, I.R. , Merz, K.M., Ferguson, D.M., Spellmeyer, D.C., Fox, T., Caldwell, J.W. , Kollman, P.A.:A second generation force field for the simulation of proteins, nucleic acids, and organic molecules, *Journal of the American Chemical Society*,**1995**, **117**, 5179-5197.
[20] Weiner, S.J. , Kollman, P.A., Case, D.A., Singh, U.C., Ghio, C., Alagona, G., Profeta, S., Weiner, Jr. P.: New Force Field for Molecular Mechanical Simulation of Nucleic Acids and Proteins, *Journal of the American Chemical Society*, **1984**, **106**, 765–784.
[21] Minini, L., Alvarez, G., Gonzalez, M., Cerecetto, H., Merlino, A.: Molecular docking and molecular dynamics simulation studies of Trypanosoma cruzi triosephosphate isomerase inhibitors, Insights into the inhibition mechanism and selectivity, *Journal of Molecular Graphics and Modelling*, **2015**, **10**, 1016.

[22] Tripathi, A., Misra, K.: Molecular Docking: A Structure-Based drug designing approach, *JSM Chemistry*, **2017**, **5**, 1042.
[23] Trott, O., Olson, A.J.: AutoDock Vina, Improving the speed and accuracy of docking with a new scoring function, efficient optimization and multithreading, *Journal of Computational Chemistry*, **2010**, **31**, 455-461.
[24] Moroy, G., Martiny, V.Y., Vayer, P., Villoutreix, B.O., Miteva M.A.: Toward in silico structure-based ADMET prediction in drug discovery, *Drug Discovery Today*, **2012**, **17**, 44-55.
[25] Gillespie, S.H.: Medical microbiology-Illustrated. Butterworth Heinemann LTD, UK.234, **1994**.
[26] Salimon, J., Salih, N., Ibraheem, H., Yousif, E.: Synthesis of 2-N-salicylidene-5-(substituted)-1,3,4-thiadiazole as potential antimicrobial agents, *Asian Journal* of *Chemistry*, **2010**, **22**, 5289-5296.
[27] Salih, N., Salimon, J., Yousif, E.: Synthesis and antimicrobial activities of 9H-carbazole derivatives, *Arabian Journal* of *Chemistry*, **2016**, **9**, S781-S786;
[28] Rao, V.B., Prasad, K.G., Naragani, K., Muvva, V.: Screening and antimicrobial activity of actinomycetes isolated from the rhizosphere of Clitoria ternatea, *Journal of Nature and Natural Sciences*, **2016**, **1** ,1-4.
[29] HyperChem (Molecular Modeling System) Hypercube, Inc., 1115 NW, 4th Street, Gainesville, FL 32601, USA, 2008.
[30] Ryckaert, J.P., Ciccotti, G., Berendsen, H.J.C.: Numerical integration of the Cartesian equations of motion of a system with constraints: molecular dynamics of n-alkanes, *Journal of Computational Physics*, **1977**, **23**, 327-341.
[31] Humphrey, W., Dalk, A., Schulten, K.: VMD: Visual Molecular Dynamics, *Journal of Molecular Graphics and Modeling*, **1996**, **14**, 33-38.
[32] Case, D.A., Darden, T.A., Cheatham, T.E.III., Simmerling, C.L. , Wang, J., Duke, R.E., Luo, R. , Walker, R.C., Zhang, W., Merz, K.M., Roberts, B., Wang, B., Hayik. S., Roitberg, A., Seabra, G., Kolossváry, I. , Wong, K.F., Paesani, F. , Vanicek , J. , Liu, J., Wu, X., Brozell, S.R., Steinbrecher, T., Gohlke, H., Cai, Q. , Ye, X., Wang, J., Hsieh, M.J., Cui, G., Roe, D.R. , Mathews, D.H., Seetin, M.G. , Sagui, C., Babin, V., Luchko, T ., Gusarov, S. , Kovalenko, A., Kollman, P.A. ,AMBER 11.University of California, San Francisco, 2010.
[33] Daoud, I., Mesmoudi, M., Ghalem, S.: Studies on binding modes between salivary amylase-food dyes and effect of Copper ions: molecular docking approach, *Der Pharma Chemica*, **2012**, **4**, 1594-1602.
[34] http://www.rcsb.org/pdb, 3G75and 2XTK, Protein Data Bank (PDB) Biological Macromolecular Resource.
[35] http://molegro.com/mvd-product.php.
[36] Bursulaya, B.D., Totrov, M., Abagyan, R., Brooks, C.L.: Comparative study of several algorithms for flexible ligand docking, *Journal* of *Computer-Aided Molecular* Design, **2003**, **17**, 755–763.
[37] Ouassaf, M., Belaidi, S., Lotfy, K., Daoud, I., Belaidi, H.: Molecular Docking Studies and ADMET Properties of New 1.2.3-Triazole Derivatives for Anti-Breast Cancer Activity, *Journal of Bionanoscience*, **2018**, **12**, 1–11.
[38] Anuf, A.R., Ramaraj, K.: Inhibition of FGFR2 signal transduction in Acne Vulgaris using Bioactive Flavonoids: An In silico approach, *Journal of Medical and Pharmaceutical Sciences*, **2014**, **2**,136–142.
[39] Laskowski, R.A., Swindells, M.B.: LigPlot: Multiple ligand-protein interaction diagrams for drug discovery, *Journal of Chemical Information and Modeling*, **2011**, **51**, 2778-2786.
[40] Lipinski, C. A.: Lead- and drug-like compounds: the rule-of-five revolution, *Drug Discovery. Today: Technologies*, **2004**, **1**, 337-341.
[41] Ghose, A. K., Viswanadhan, V.N., Wendolowski, J.J.: A knowledge-based approach in designing combinatorial or medicinal chemistry libraries for drug discovery, 1: A qualitative characterization of known drug databases, *Journal of Combinatorial Chemistry*, **1999**, **1**, 55-67.

[42] Veber, F. D., Johnson, S.R., Cheng, H.Y., Smith, B. R., Ward, K. W., Kopple, K. D.: Molecular properties that influence the oral bioavailability of drug candidates, *Journal of Medicinal Chemistry*, **2002**, **45**, 2615-2623.
[43] Cheng, F., Li, W., Zhou, Y., Shen, J., Wu, Z., Liu, G., Lee, P.W., Tang, Y.: ADMET SAR: a comprehensive source and free tool for assessment of chemical ADMET properties, *Journal of Chemical Information and Modeling*, **2012**, **52**, 3099-3105.
[44] Khamouli, S., Belaidi, S., Lanez, T.: Molecular docking and ADMET studies of amino-pyrimidine derivatives as mycobacterium tuberculosis SER/THR protein kinases b inhibitors, *Journal of Fundamental and Applied Sciences*, **2019**, **11**, 914-939;
[45] Imberty, A., Hardman, K.D., Carver, J.P., Pérez, S.: Molecular of protein carbohydrate interactions. Docking of monosaccharides in the binding site of concanavaline A, *Journal of Glycobiology*, **1991**, 1, 631-642;
[46] A. Jay, Bemis, G.W., Murcko, M.A.: Designing libraries with CNS activity, *Journal of Medicinal Chemistry*, **1999**, **42**, 4942–4951.